Dynamics of Deep-Bed Filtration

Part II: Experiment

Filtration experiments were conducted using granular beds composed of nearly monosized filter grains and monodispersed suspensions. The experimental data obtained are histories of filtrate quality and pressure drop across the filter bed, from which local filter coefficient and pressure gradient were determined as functions of the specific deposit. The experimental results, together with the results of the analyses of the two limiting situations presented in Part I, were used to develop a general correlation which accounts for the change in filter performance caused by particle deposition.

HSU-WEN CHIANG
and CHI TIEN

Department of Chemical Engineering and
Materials Science
Syracuse University
Syracuse, NY 13210

SCOPE

The experimental work reported in this paper concerned the effect of particle deposition on filter performance and was conducted with a relatively shallow bed composed of nearly monosized glass spheres. Lycopodium and ragweed particles were used to prepare the test suspensions. Both the electrophoretic mobility measurements as well as the initial collection efficiency values obtained experimentally suggested that the particle-filter grain surface interactions were not adverse. The results obtained from the experiments are the effluent concentration history and the history of the pressure drop across the filter bed for a given flow rate.

A quantitative assessment of the effect of particle deposition on filter performance requires knowledge of the filter coefficient and the required pressure gradient for a given flow rate as functions of the extent of particle deposition in filter bed; in other words, one must know the specific deposit. To obtain such information from the data on filtrate quality history or pressure drop history, an optimization-search technique was developed. Application of this technique to experimental data obtained in this study makes it possible to assess the validity of using the two limiting situations to describe deep-bed filtration.

By comparing the experimental results with the results from the analyses of the two limiting situations, an empirical correlation was developed relating the change of filter coefficient with the extent of deposition and other operating variables, thus making the prediction of the dynamic behavior of deep-bed filtration a more likely reality.

CONCLUSIONS AND SIGNIFICANCE

Experimental results on the filtration of an aqueous suspension of lycopodium and ragweed particles through packed beds of glass spheres demonstrate that both the filter coefficient and the pressure gradient necessary to maintain a given flow rate increase with the increase in the specific deposit, σ, and can be expressed as a simple power function of σ and as an exponential function of σ, respectively. In addition, the initial filter coefficient, λ_o, was found to agree with both the correlation of Rajagopalan and Tien (1976) and the trajectory analysis results using the constricted-tube model for media characterization.

Although the experimentally observed change in the filter coefficient with the increase of particle deposition does not agree with the analytical results corresponding to the two limiting situations presented in Part I, it was found possible to approximate the experimental data by combining the results of these two limiting situations. The use of this procedure can be defended on the basis that the morphology of deposits formed in a clogged filter bed is not simple but covers a variety of geometries, including those corresponding to the two limiting situations discussed in Part I. The correlation obtained relates the increase in the filter coefficient to two variables: the specific deposit, and the relative size parameter, defined as the diameter ratio of particle to filter grain. The validity of this correlation is further tested against the recently available data of Vigneswaran (1980) and Tanaka (1982). In the absence of any general correlation of the change of filter coefficient with the particle condition, the result presented here can be used to predict the transient behavior of deep-bed filtration for cases of favorable surface interaction and no appreciable particle reentrainment.

Hsu-Wen Chiang is currently with Whiteshell Nuclear Research Establishment, Atomic Energy of Canada Ltd., Pinawa, Manitoba, R0E 1L0, Canada.

INTRODUCTION

Experimental work on deep-bed filtration conducted in the past has shown that both the filtration quality of the filber bed and the pressure drop across the bed necessary to maintain a constant flow rate change with time. Since the quality of filtrate obtained in a filter bed is a direct consequence of the extent of particle removal achieved in the bed, characterized by the value of filter coefficient, the change in particle removal can be expressed by the change in the filter coefficient with the extent of particle deposition, σ. Similarly, one may describe the pressure drop change in terms of the change of the local pressure gradient with σ. Mathematically, the effect of particle deposition on filter performance can be described by two functions, F_1 and F_2, defined as

$$\frac{\lambda}{\lambda_o} = F_1(\alpha,\sigma) \tag{1}$$

$$\frac{\partial p/\partial z}{(\partial p/\partial z)_o} = F_2(\beta,\sigma) \tag{2}$$

In principle, the functions F_1 and F_2 can be obtained from theoretical analysis based on knowledge of the flow field around filter grains, the trajectories of particles in the liquid phase, the nature and magnitude of the surface interactions between particles and filter grains, and their changes with time as the extent of deposition increases. Such a complete analysis is impossible, or at least impractical, at present. Instead, theoretical analysis is limited to simplified, idealized model situations, as in Part I. Similarly, one may identify the functional form of F_1 (or F_2) empirically from a large body of experimental data covering wide ranges of relevant variables. The collection of filtration data under well-defined and controlled conditions, however, is a tedious undertaking because of the very large number of variables involved and the significant uncertainties associated with particle counting. Furthermore, even in a very shallow bed (for example, with a bed height one order of magnitude larger than the grain dimension), one may expect significant variations of the extent of particle deposition along the axial direction. The extraction of values of F_1 (or F_2), which is a local function from experimental data such as effluent concentration or pressure drop, inevitably introduces errors and uncertainties. As a result, empirically determined F_1 and F_2 in general have only limited utility. Applying F_1 (or F_2) obtained under one set of conditions to different sets of conditions is not considered advisable.

The purpose of the present work was not to obtain another limited correlation to account for the effect of particle deposition on filter performance. The experimental data were obtained to be compared with the results of the two limiting situations discussed in Part I. More important, however, is that through a combination and comparison of these experimental and theoretical results, one may obtain a more general correlation on the effect of particle deposition. This combination approach was used successfully in an earlier effort for obtaining the initial collection efficiency of aerosol filtration in granular beds (Pendse and Tien, 1982).

EXPERIMENTAL

Apparatus

A schematic diagram of the experimental apparatus is shown in Figure 1. The main components of the apparatus included a suspension preparation tank, a pump, an overflow constant-head tank, and an experimental filter. The suspension preparation tank had a mechanical mixer and an ultrasonic dismembrator (Model 150, Artek Systems Corp., Farmingdale, NY) inside the tank to keep suspended particles from settling and agglomerating. A Masterflex[B] tubing pump (Cole-Parmer Instrument Company, Chicago, IL) was used to deliver suspensions. The overflow constant-head tank was a square column, 240 mm high and 50 mm wide. A mechanical stirrer inside the column was used to keep particles uniformly suspended.

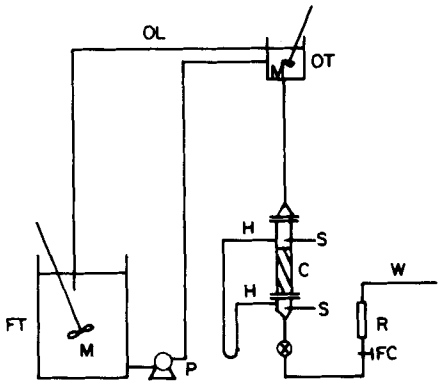

C - FILTER COLUMN
FC - FLOW RATE CONTROLLER
FT - SUSPENSION MIXING TANK
H - PRESSURE TAP
M - MECHANICAL MIXER
OL - OVERFLOW LINE
OT - OVERFLOW TANK
P - PUMP
R - ROTAMETER
S - SAMPLING TAP
W - WASTE LINE

Figure 1. Schematic diagram of the experimental apparatus.

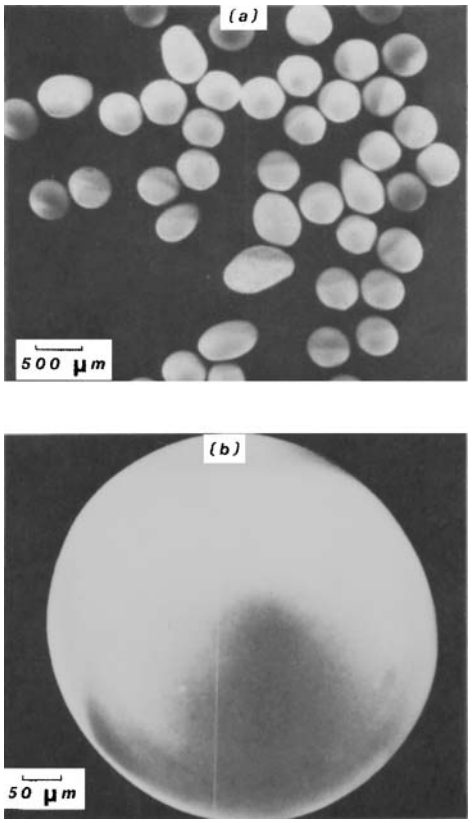

Figure 2. Scanning electron micrographs of glass beads.

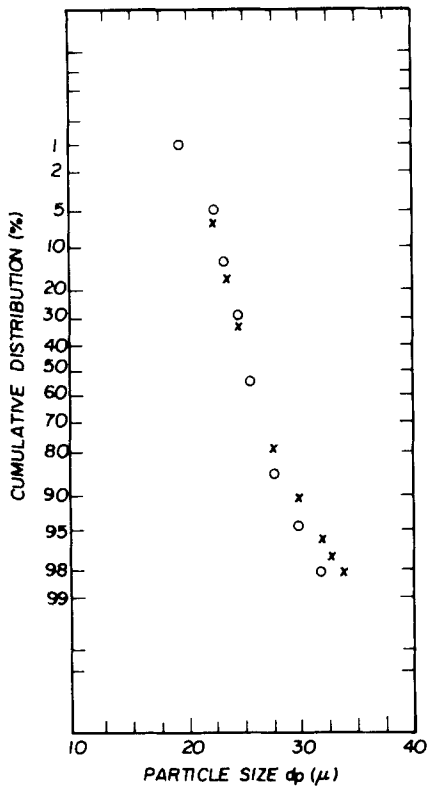

Figure 3. Size distribution (by volume) of lycopodium particles.

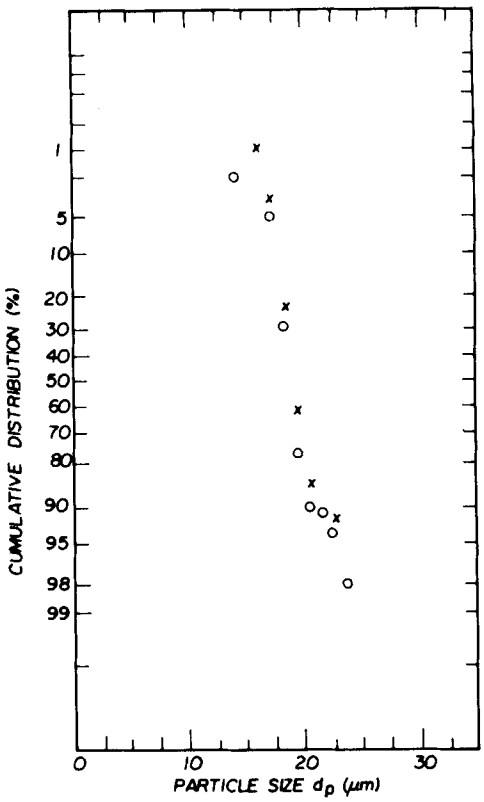

Figure 5. Size distribution (by volume) of ragweed particles.

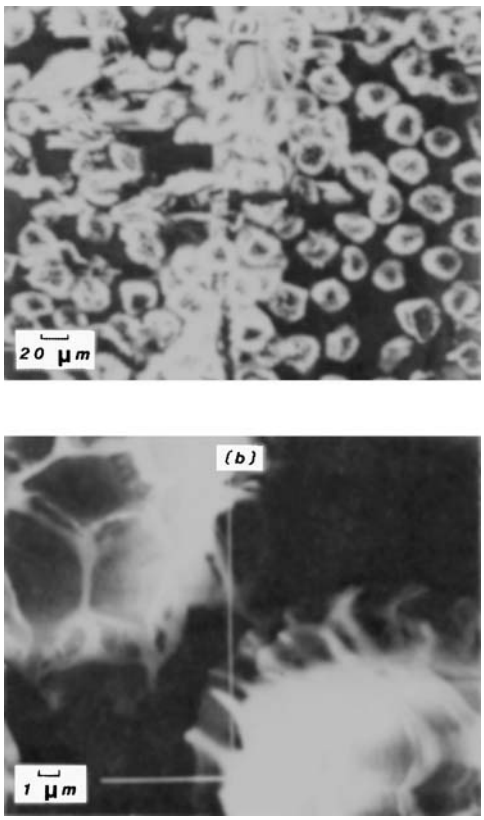

Figure 4. Scanning electron micrographs of lycopodium particles.

The experimental filter, made of a Plexiglass cylinder 25.4 mm in diameter, was placed 1.15 m below the overflow constant-head tank. A divergent funnel preceded the inlet to the filter to insure that a flat velocity profile within the filter could be realized. Also, a screen was placed at the lower section of the filter as a filter grain support. Two pressure taps were located, respectively, at 20 mm below the divergent funnel and 35 mm below the screen support. Sampling tubes, one influent and one effluent, were placed 30 mm below the funnel and 0.1 m below the support screen, respectively. The distance between the influent sampling tube and the screen was 50 mm.

Experimental Systems

Filter Grains. Glass beads classified by U.S. No. 30 and 40 sieves were used as filter grains. The size distribution of these glass beads was very narrow, with an average diameter of 505 μm. The scanning electron micrographs of the glass beads (Figure 2) show that the size and shape of the glass beads were reasonably uniform and that their surfaces were very smooth.

Suspended Particles. The suspended particles used in this study were lycopodium and ragweed. The lycopodium particles were obtained from Galland-Schlesinger Chemical Manufacturing Corp. (Carle Place, NY). The size distribution of the particles measured by a Coulter counter (Model ZB, Coulter Electronics, Inc., Hialeah, FL) is shown in Figure 3. These particles were nearly monodispersed. The median diameter of the particles was 26 μm, and 90% (by volume) of the particles were in the range of 22.5 to 30.5 μm. The scanning electron micrographs of the lycopodium particles are shown in Figure 4. The shape of the lycopodium particles can be described as more or less spherical, with needles sticking out from the surface of the sphere. The length of a needle was approximately 3 μm.

The ragweed particles were obtained from the Sigma Chemical Co. (St. Louis, MO). The size distribution of the particles is shown in Figure 5. The median diameter of the particles was 19.5 μm, with 90% of the particles in the range of 18 to 23 μm. The scanning electron micrographs of the ragweed particles are shown in Figure 6. The ragweed particles looked like spheres, with protrusions (approximately 1 μm in length) on the surface of the sphere.

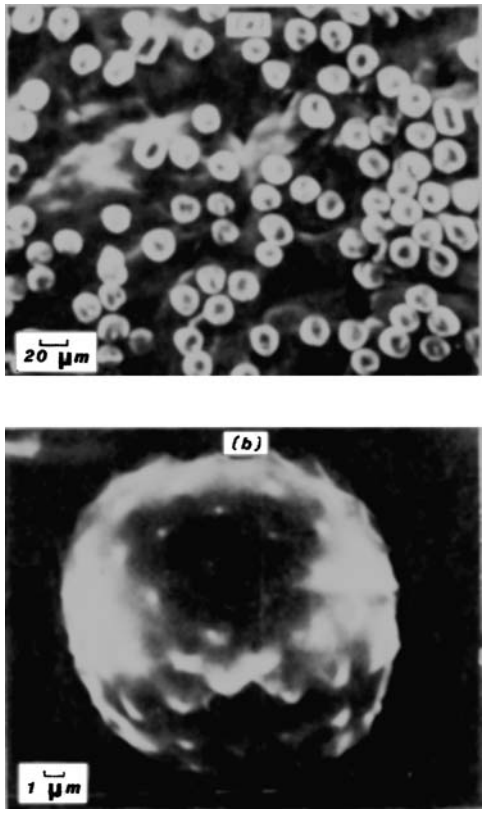

Figure 6. Scanning electron micrographs of ragweed particles.

The electrophoretic mobility of both the lycopodium and ragweed particles in aqueous suspensions used in the experiments was measured by means of a Rank Electrophoresis Unit with a rectangular cell (Rank Brothers, Ltd., Cambridge, England). Under the conditions of a pH value of 6 and an ionic concentration of 10^{-6} M NaCl, the average value of twenty measurements of the electrophoretic mobility was used to obtain the zeta potential. The zeta potential of the lycopodium particle suspension was −37 mv and that of the ragweed particle suspension was −17 mv.

Experimental Procedures

Preparation of Suspensions. To prepare the test suspensions, a suitable number of particles, together with distilled water, were added to a 200 mL flask. The flask was thoroughly shaken and then placed in an ultrasonic cleaner (Heat Systems-Ultrasonic, Inc., Plainview, NY) to insure the absence of flocculation. The suspension, with a pH value of around 6, was then introduced into the mixing tank, with distilled water added to obtain the desired particle concentration. An ultrasonic dismembrator and a mechanical mixer were used to keep the particles uniformly suspended.

Preparation of Filter Bed. Before each filtration run, the filter was packed with fresh glass beads to the specified height. Then water was pumped into the bed from the bottom of the filter to fluidize the bed and insure that no gas bubble was present in the filter. The porosity of the filter bed was found to be 0.41.

Filtration Run. To start an experiment, the suspension was prepared in the mixing tank, pumped to the constant-head tank, and passed into the filter, which was packed with glass beads to specified height. The flow rate was kept constant by adjusting a valve placed before the rotameter. Influent and effluent samples were taken at specific intervals beginning a few minutes after the start of the experiment. This time lapse was necessary in order to assure a total displacement by the test suspension of the clean water initially present in the filter.

Determination of Particle Concentration. The particle concentration and size distribution of samples taken were determined using a Coulter counter equipped with a multichannel analyser (Model C-1000) and interfaced with an Apple II-Plus computer. The counter was calibrated with 9.8 μm polystyrene DVB particles and 2.02 μm polystyrene particles supplied by Particle Information Service Inc. (Kingston, WA) and Coulter Electronics Inc., (Hialeah, FL), respectively.

Measurement of Pressure Drop. The pressure drop across the bed was measured by a U-tube manometer filled with carbon tetrachloride.

EXPERIMENTAL RESULTS

The experimental conditions for the work conducted are listed in Table 1. Lycopodium particles were used in the first four experimental runs, with the major difference in the experimental conditions of these four runs being the filtration velocity. Ragweed particles were used in experimental run No. 5. Experimental run No. 6 was intended to show the effect of bed height on particle collection and pressure drop.

The experimental results from each filtration run consisted of the effluent quality and pressure drop at various times, a typical set of which is shown in Figure 7. The experimental accuracy of the concentration measurements is indicated by the error bar on Figure 7a and depends mainly on the number of particles counted by the Coulter counter. For influent samples, the particle counts per Coulter counter sample numbered approximately 200, with the accuracy of the measurements about 7%. For effluent samples, the particle counts per Coulter counter sample were fewer than 200 and the accuracy of the measurements greater than 7%. In general, the accuracy of the concentration ratio of effluent to influent was about 15%. Normally, the concentration ratio decreases with the increase in filtration time. Some occasional small mag-

TABLE 1. SUMMARY OF EXPERIMENTAL CONDITIONS USED IN THIS WORK

	Run Number					
	1	2	3	4	5	6
Filter medium	Glass	Glass	Glass	Glass	Glass	Glass
Particles in suspension	Lycopodium	Lycopodium	Lycopodium	Lycopodium	Ragweed	Lycopodium
Bed porosity	0.41	0.41	0.41	0.41	0.41	0.41
Superficial velocity u_s, cm/s	0.1	0.2	0.27	0.4	0.1	0.1
Grain diameter d_g, cm	0.0505	0.0505	0.0505	0.0505	0.0505	0.0505
Particle diameter d_p, cm	0.0026	0.0026	0.0026	0.0026	0.00195	0.0026
Bed height L, cm	0.5	0.5	0.5	0.5	0.5	1.0
Feed concentration c_{in}, ppm	9.0	5.0	27.0	6.0	12.0	6.0

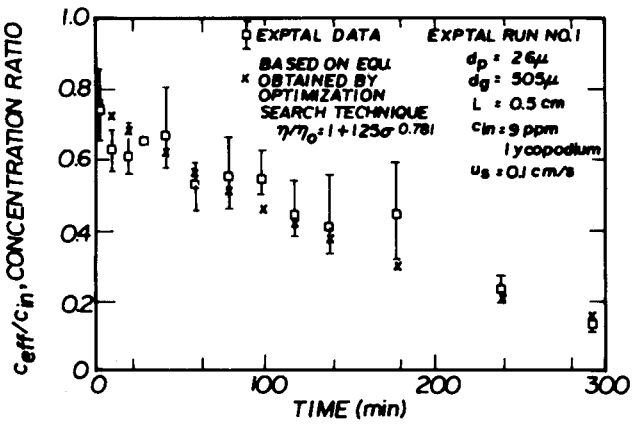

Figure 7a. Ratio of effluent concentration to influent concentration vs. filtration (experimental Run No. 1).

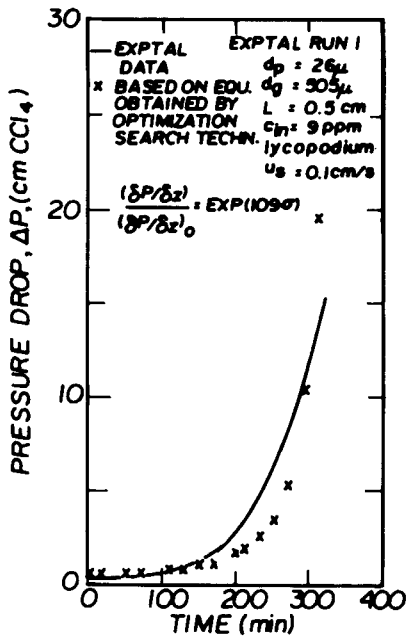

Figure 7b. Pressure drop vs. filtration time (experimental Run No. 1).

nitude oscillations of the concentration ratio were observed, however. On the other hand, pressure drop across the bed always increased with time; the slope (i.e., $\partial(\Delta p)/\partial t$) also increased with time.

Interpretation of Experimental Results

The results of the analysis presented in Part I were expressed in terms of the change in unit collector efficiency and pressure gradient as functions of σ for a given set of operating variables. The experimental data obtained are in the form of the effluent quality and pressure drop, Δp, across the bed. Described below are the procedures used in extracting information from the experimental data so that a comparison between experiments and theoretical analyses can be made.

The effect of particle deposition on filter performance can be expressed as

$$F_1(\alpha,\sigma) = \frac{\lambda}{\lambda_o} = \frac{\eta}{\eta_o} \tag{3}$$

where α and η are the filter coefficient and the collection efficiency of the unit collector, respectively. The subscript o refers to the initial state. λ and η are related to each other by the expression (Tien and Payatakes, 1979)

$$\lambda = \frac{1}{\ell}\ln\frac{1}{1-\eta} \simeq \eta/\ell \tag{4}$$

where ℓ is the axial bed distance occupied by a unit collector. ℓ is given as (Payatakes et al., 1973):

$$\ell = \left[\frac{\pi}{6(1-\epsilon)}d_g^3\right]^{1/3} \tag{5}$$

A filter bed of depth L may be considered to be composed of $N(=L/\ell)$ unit collectors connected in series. Let c_i denote the particle concentration of the suspension leaving the ith unit collector. The ratio of the effluent to the influent concentration can be expressed as

$$c_{eff}/c_{in} = \prod_{i=1}^{N}(c_i/c_{i-1}) = \prod_{i=1}^{N}(1-\eta_i) = \prod_{i=1}^{N}\{1-(\eta_i)_o F_1(\alpha,\sigma_i)\} \tag{6}$$

For a homogeneous filter bed, $(\eta_i)_o$ is the same throughout the bed. The ratio c_{eff}/c_{in} becomes

$$c_{eff}/c_{in} = \prod_{i=1}^{N}[1-\eta_o F_1(\alpha,\sigma_i)] \tag{7}$$

The extent of particle deposition is described by σ, the specific deposit. Let σ_i denote the specific deposit of the ith collector. By material balance over the ith collector, one has

$$\sigma_i = \int_0^\theta \frac{u_s}{\ell}(c_i - c_{i-1})d\theta \tag{8}$$

where u_s is the superficial velocity and θ the corrected time.

Substituting Eq. 7 into the differentiated form of Eq. 8, one has

$$d\sigma_n/d\theta = \frac{u_s}{\ell}\eta_o F_1(\alpha,\sigma_n)\prod_{i=1}^{n-1}[1-\eta_o F_1(\alpha,\sigma_i)] \tag{9}$$

Equation 9 with the initial conditions

$$\sigma_n = 0 \text{ at } \theta = 0 \text{ for } n = 1, 2, \ldots N \tag{10}$$

forms a set of N ordinary differential equations, the solutions of which give the values of σ_i vs. θ for all the unit collectors of which the bed was composed.

From the experimental results, the concentration ratio, c_{eff}/c_{in}, at various times is known, and $N = L/\ell$ is specified. The problem is to determine the functional form of F_1. Toward this end, an objective function, ϕ_c, is defined as

$$\phi_c = \prod_{m=1}^{M} w_m[(c_{eff}/c_{in})_{\text{expt},m} - (c_{eff}/c_{in})_{\text{pred},m}]^2 \tag{11}$$

where M is the number of data points. w_m's are the weighting factors associated with the mth data point. w_m may be assigned to $1/\delta_m^2$, where δ_m is the experimental error associated with each data point. This choice was made on the grounds that the weight assigned to each datum in determining F_1 should be inversely proportional to its accuracy.

Determining F_1 from experimental data is reduced to an optimization-search problem, namely, F_1 is found on the condition which gives ϕ_c a minimum. In actual practice, a given functional form of F_1 is specified first. For example, as one possibility, F_1 may be assumed to be

TABLE 2. PARAMETER VALUES OF α AND β OBTAINED BY OPTIMIZATION SEARCH TECHNIQUE FROM EXPERIMENTAL DATA

Run No.	α_1^*	α_2^*	α_1^{**}
1	125	0.781	109
2	152	0.952	158
3	208	1.03	27.3
4	10.8	0.417	89.3
5	26.8	0.569	86.2

* Based on functional form $F_1(\alpha,\sigma) = 1 + \alpha_1\sigma^{\alpha_2}$.
** Based on functional form $F_2(\beta,\sigma) = \exp(\beta\sigma)$.

$$F_1 = 1 + \alpha_1\sigma^{\alpha_2} \tag{12}$$

The coefficient and exponent are to be determined on the basis of yielding a minimum of the objective function ϕ_c. The search was performed using the algorithm ORGLS (a general Fortran least-square program, Oak Ridge National Laboratory, Oak Ridge, TN). The algorithm is based on the Gauss-Newton method and considers that, at the optimum, the partial derivative of the objective function with respect to each searched parameter should be equal to zero. The algorithm can adjust the parameters of an arbitrary function in order to fit a set of observed values by the method of least squares. The derivatives required are either obtained numerically by the program or calculated analytically by the user's subroutine.

The calculated values of c_{eff}/c_{in} were obtained from the solution of Eqs. 7, 9, and 10. The integration of Eq. 9 was made using the algorithm EPISODE (Effective Package for the Integration of System of Ordinary Differential Equations), which is a slightly modified version of the Gear package for solving ordinary differential equations (ODE). Once σ_i vs. θ was known for $i = 1, 2, \ldots N$; the effluent to influent concentration ratio, $(c_{eff}/c_{in})_{\text{pred}}$ was found from Eq. 7, with F_1 given by Eq. 12, which in turn was used to calculate the objective function, ϕ_c.

A similar procedure was used to determine F_2 from the pressure drop data. By considering that a bed of height L is equivalent to $N\ (= L/\ell)$ unit collectors connected in series and the definition of $F_2\ (= \Delta p/\Delta p_o)$, one has

$$(\Delta p/L)/(\Delta p/L)_o = \frac{1}{N}\sum_{i=1}^{N} F_2(\beta,\sigma_i) \tag{13}$$

and

$$F_2 = \exp(\beta,\sigma) \tag{14}$$

where the subscript o denotes the initial, or clean collector state; σ_i, the specific deposit of the ith unit collector, can be found from the solution of Eqs. 9 and 10. The corresponding objective function, ϕ_p, becomes

$$\phi_p = \sum_{m=1}^{M} w_m \left[\left\{\frac{\Delta p/L}{(\Delta p/L)_o)}\right\}_{\text{expt},m} - \left\{\frac{\Delta p/L}{(\Delta p/L)_o}\right\}_{\text{pred},m}\right]^2 \tag{15}$$

In other words, the function F_2 is determined by minimizing the objective function from the pressure data.

By applying the aforementioned optimization-search procedures for each experimental run, one obtains the functional form of λ/λ_o (or η/η_o) and $(\partial p/\partial z)/(\partial p/\partial z)_o$ (or F_1 or F_2) as well as the associated parameter values of α and β.

Table 2 presents the results of F_1 and F_2 obtained from experimental data of filtrate quality and pressure drop by applying the optimization-search procedure. There does not appear a simple relationship between the parameters (α_1, α_2, or β) and the operating variables. With the use of values shown in Table 2 and Eqs. 7, 8, 10, and 13, the effluent concentration and pressure drop across the filter bed can be obtained and are expressed by the symbol "x" in Figures 7a,b. Generally speaking, agreement between the experiments and predictions is fairly good.

COMPARISON OF EXPERIMENT WITH THEORIES

Initial Collection Efficiency

Theoretical predictions of the initial collection efficiency can be made with the trajectory analysis; this has been a subject of intense interest during the past decade. As pointed out by Rajagopalan and Tien (1979), regardless of the specific collector geometry used in the analysis, the results were found largely comparable. For the present comparison, the correlation used was that of Rajagopalan and Tien (1976), which is based on their numerical results obtained with the use of Happel's sphere-in-cell model and favorable surface interactions between filter grain and particle. In addition, the trajectory analysis results using a sinusoidal constricted-tube (SCT) geometry and assuming that interception is the only mechanism were also compared with the data. Rajagopalan and Tien's correlation is expressed as:

$$\eta_o = (1-\epsilon)^{2/3}A_s N_{Lo}^{1/8} N_R^{15/8} + 3.375\times 10^{-3}(1-\epsilon)^{2/3}A_s N_G^{1.2} N_R^{-0.4} + 4A_s^{1/3}N_{Pe}^{-2/3} \tag{16}$$

For the trajectory calculation in an SCT with interception the collection mechanism, η_o is given as

$$\eta_o = \frac{\psi^*|_{z^*=0.5,P^*=(d_c^*-N_R)/2} - \psi^*|_{z^*=0,P^*=P_o^*}}{\psi^*|_{z^*=0,P^*=0} - \psi^*|_{z^*=0,P^*=P_o^*}} \tag{17}$$

This equation is a special case of Eq. 23 of Part I. In other words, Eq. 17 corresponds to Eq. 23 of Part I when the constricted tube is free of deposits. Chow and Soda's (1972) flow field solution within a constricted tube can readily be used to determine the values of the stream function.

The comparisons between the experimental and theoretical results on the initial collection efficiency are shown in Table 3. Also included in this table are recent experimental results by Vigneswaran (1980) and Tanaka (1982) as well as earlier results of Adin and Rebhun (1974). Generally speaking, agreement between the experimental data and the theoretical results is reasonably good, especially in view of the inherent uncertainties associated with determining λ. Vigneswaran's data, on the other hand, were found to be significantly higher (up to one order of magnitude) than theoretical results.

Effect of Particle Deposition on Particle Collection

Figures 8a, b, and c show the comparison between the relationship of F_1 vs. σ obtained from applying the optimization-search to experimental data of filtrate quality and those obtained from analyses of the two limiting situations discussed in Part I. Also included in the figure is the prediction based on the phenomenological model of Tien et al. (1979). The results of this comparison as well as similar comparisons made as part of this study demonstrate that the experimentally derived F_1 in all cases disagrees with the theories considered. On the one hand, both the phenomenological model (Tien et al., 1979) and the results corresponding to limiting case (A) of Part I underestimate F_1. The premise used in limiting case (A) is that collected particles form smooth deposits. Similarly, the phenomenological model of Tien et al. (1979) considers the morphology of particle deposits formed as that of a smooth coating. In either case, the effect of deposited particles acting as additional particle collectors is minimized. The fact that both theories yield results which are lower than experiments is, therefore, not unexpected.

On the other hand, the stochastic model [limiting case (B) of Part

TABLE 3. COMPARISONS OF EXPERIMENTAL DATA WITH THEORETICAL RESULTS CONCERNING INITIAL COLLECTION EFFICIENCY

Experimenter and Run No.	Experimental Value	Theory (a)*	Theory (b)**
This work			
1	2.820×10^{-2}	8.800×10^{-2}	2.390×10^{-2}
2	2.430×10^{-2}	8.800×10^{-2}	2.160×10^{-2}
3	1.910×10^{-2}	8.800×10^{-2}	2.070×10^{-2}
4	2.970×10^{-2}	8.800×10^{-2}	1.970×10^{-2}
5	1.587×10^{-2}	5.240×10^{-2}	1.500×10^{-2}
Vigneswaran (1980)			
1	1.057×10^{-2}	1.108×10^{-3}	6.190×10^{-4}
2	1.560×10^{-2}	4.329×10^{-3}	1.934×10^{-3}
3	3.080×10^{-2}	1.097×10^{-2}	4.508×10^{-3}
4	5.900×10^{-3}	4.368×10^{-4}	4.329×10^{-4}
5	1.017×10^{-2}	1.721×10^{-3}	1.443×10^{-3}
6	1.448×10^{-2}	4.410×10^{-3}	3.515×10^{-3}
7	1.385×10^{-2}	1.108×10^{-3}	6.190×10^{-4}
8	6.820×10^{-3}	1.108×10^{-3}	4.545×10^{-4}
9	7.304×10^{-3}	1.108×10^{-3}	6.190×10^{-4}
Tanaka (1982)			
41	2.914×10^{-3}	1.026×10^{-3}	1.906×10^{-3}
19	2.982×10^{-3}	1.026×10^{-3}	1.906×10^{-3}
30	1.837×10^{-3}	1.026×10^{-3}	1.906×10^{-3}
16	1.567×10^{-3}	1.026×10^{-3}	1.906×10^{-3}
Adin and Rebhun (1974))	3.177×10^{-3}	2.003×10^{-3}	2.557×10^{-3}

* Trajectory calculation in an SCT; the deposition mechanism considered was interception alone.
** Based on Rajagopalan and Tien (1976).

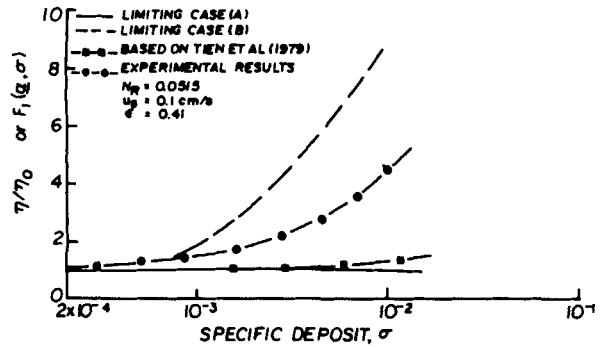

Figure 8a. Comparison of predicted relationship between F_1 and σ with experimental results: Run No. 1.

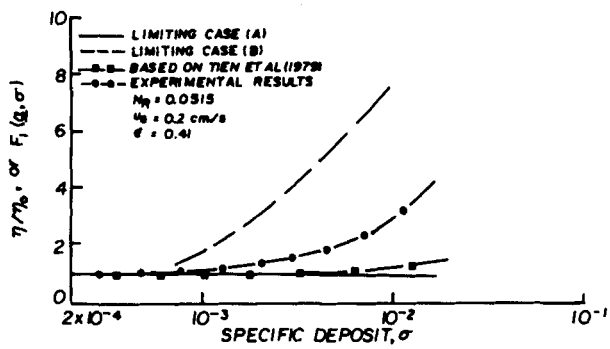

Figure 8b. Comparison of predicted relationship between F_1 and σ with experimental results: Run No. 2.

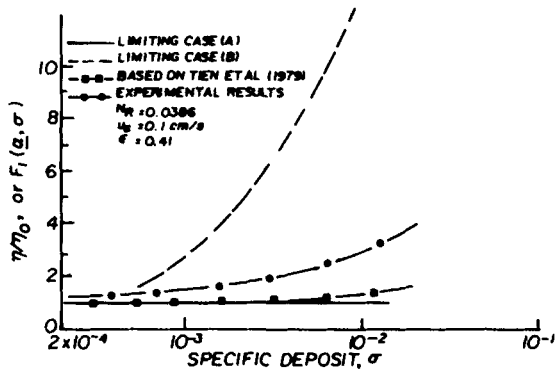

Figure 8c. Comparison of predicted relationship between F_1 and σ with experimental results: Run No. 5.

I] overestimates F_1. For the stochastic model [limiting case (B)], particle aggregates, once formed, are assumed to remain unchanged. In reality, as the particle deposit grows, the hydrodynamic drag force acting on particle deposits increases. As a result, it is likely that some of the deposits may bend and experience a slow creeping or kneading action, which will spread the deposited material over the collector. This occurrence tends to create a smooth coating. In that event, the extent to which deposited particles may act as particle collectors is reduced. Therefore, one may expect that the stochastic model [limiting case (B)], which neglects bending, creeping, and kneading of the deposited material, will overestimate F_1. From the experimental data, the actual process of particle deposition is neither one that involves only a smooth coating [limiting case (A)] nor one limited to undisturbed, that is, "unbent" particle aggregates [limiting case (B)]. Thus, the fact that the experimental data fall between those of the two limiting cases is not surprising.

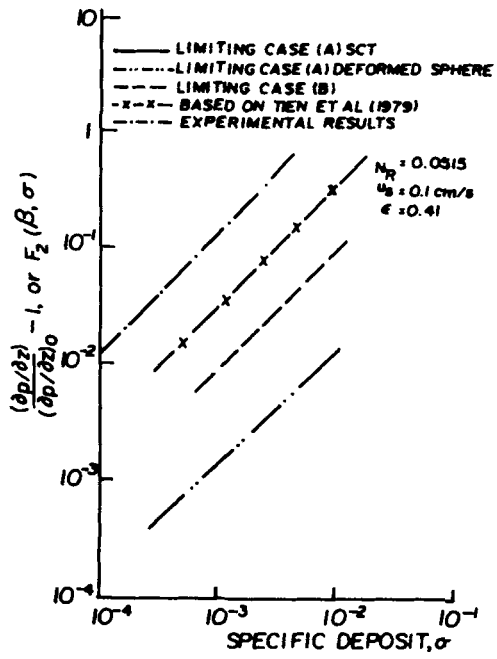

Figure 9. Comparison of predicted relationship between $F_2 - 1$ and σ with experimental results (Run No. 1).

Effect of Particle Deposition on Pressure Gradient

The experimentally determined relationships of F_2 vs. σ were compared with the predictions based on analyses of the two limiting situations as discussed in Part I as well as those based on the earlier phenomenological model (Tien et al., 1979). A typical example is shown in Figure 9. Both the results based on the phenomenological model and the two limiting situations were found to predict a much lower pressure drop increase than experiments actually yielded. The underestimation of the pressure gradient from the solution corresponding to limiting case (A) is understandable. The smooth coating morphology represents the most favorable situation of the flow of fluid. The underestimation by the solution of limiting case (B), on the other hand, deserves some explanations. One plausible explanation for this discrepancy is the presence of filter cake composed of deposited particles at the top surface of the filter. In conducting the experimental work, a run was terminated when filter cake was observed on top of the media. Determining exactly the onset of cake formation, however, was impractical with the present experimental set-up.

The discrepancy between experimental data and prediction based on limiting case (B) may also be partly explained by the following argument. The increase in pressure gradient is related to the drag force acting on the deposited particles. The procedure suggested by Pendse et al. (1981) was used to estimate the drag force. The method implicitly assumed that deposited particles are individually identifiable. Thus the increase in drag force can be estimated by knowing the velocity evaluated at the center of deposited particles from the flow field expression for a clean collector (or clean filter grain). As particle deposition progresses, however, the deposited matter may cover a major part of the grain surface. The effective size of the collector increases, or the cross-sectional area of the constricted tube narrows. In such a situation, it would be more reasonable to consider the system of filter grain plus deposited particles as a single entity. The use of the flow field corresponding to the clean collector, as suggested by Pendse et al. (1981), therefore becomes impractical.

DEVELOPMENT OF A GENERAL CORRELATION

In view of the lack of agreement between theories and experiments, attempts were made to develop an empirical correlation capable of predicting the effect of particle deposition on collection efficiency (i.e., F_1) based on theoretical calculations as well as on experimental results. The basic approach is similar to the one used by Pendse and Tien (1982) in their study of aerosol filtration in granular media. The physical complexities of deep-bed filtration make the problem amenable to theoretical analysis only with extreme simplification. Similarly, experimental data cannot be interpreted correctly without a theoretical framework nor the results correlated without theoretical guidance. Combination of the two offers the only pragmatic way of studying the problem.

Furthermore, just as the process for establishing a general correlation requires taking into account both theoretical and experimental data, it also involves considering the two limiting cases in combination. To illustrate, one should note the visual study of particle deposition in a two-dimensional model filter done by Payatakes et al. (1981). These investigators found that in the initial period of filtration, particles collide with filter grains, either rolling and sliding along the grain surfaces or adhering to a filter grain. The collected particles in turn act as collectors, capturing oncoming particles and thus forming particle aggregates. As filtration proceeds and as deposits throughout the filter experience increasing drag forces, the configurations of the deposits often change visibly, assuming more mechanically stable shapes. From time to time the particle aggregate was observed to creep along the grain surface until it came to the site of a grain where the drag was reduced. Occasionally, the particle aggregates broke away and reentered the stream. The reentrained particle cluster might then escape from collection or be deposited at a new site and continue to collect more particles at a relatively high rate. Such processes cannot be described by either the smooth coating [limiting case (A)] or the unbent particle aggregates [limiting case (B)].

Although, as mentioned earlier, the experimental data were found to disagree with all theories considered in this work, their comparisons, together with the observations by Payatakes et al. (1981) of the model filter, suggest that, practically speaking, the deposition process may be described by a combination of the two limiting cases according to an empirical rule. Such an empirical rule can be determined by comparing the experimental data with the results obtained from the two limiting cases. As a possibility, one may write

$$F_{1,\text{expt}} = fF_{1,(B)} + (1 - f)F_{1,(A)} \tag{18}$$

where $F_{1,\text{expt}}$ is the experimentally determined value and $F_{1,(A)}$ and $F_{1,(B)}$ are the theoretical values based on limiting cases (A) and (B), respectively. f is the combination factor.

Accordingly, for a given set of experimental values (F_1 vs. σ), one may derive the value of f vs. σ as shown in Figure 10, where the results obtained for the five experimental runs performed in this study are shown. It is obvious that f is not a simple constant factor, as one might wish. On the other hand, except for run No. 1, the values of f remain within a fairly narrow range. In fact, based on the average value of f (for a given σ) of the five runs, for $\sigma \geq 2 \times 10^{-3}$, f may be taken to be 0.25, or

$$F_1 = 0.25F_{1,(B)} + 0.75F_{1,(A)} \tag{19}$$

The results of the analyses of the two limiting situations given in Part I show that F_1 is either independent of or only slightly dependent on the filtration velocity. The only important factor is the relation size parameter, N_R. Accordingly, one may write

$$F_1 = G(\sigma, N_R) \tag{20}$$

To obtain a specific functional form based on the combination principle, the following procedure was employed. First, the relationships of $F_{1,(A)}$ and σ were obtained for three particle sizes (i.e., $N_R = 0.025$, 0.0386, and 0.0515) based on limiting case (A). Similarly, the relationships of $F_{1,(B)}$ and σ were obtained for the same three values of N_R based on limiting case (B). Next, $F_{1,(A)}$ and $F_{1,(B)}$

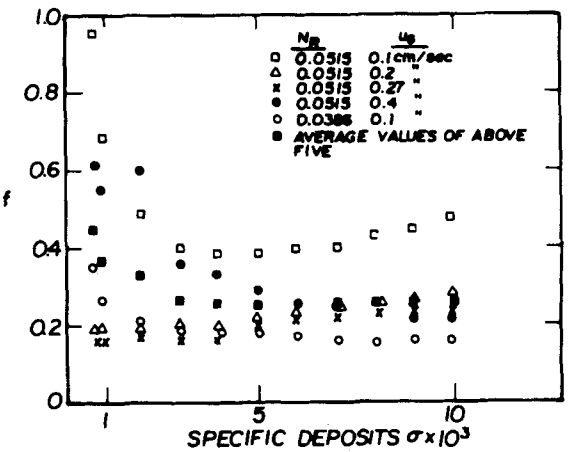

Figure 10. f vs. Specific Deposit, where f is defined as $F_{1,\text{expt}} = f \cdot F_{1(B)} + (1 - f)F_{1(A)}$.

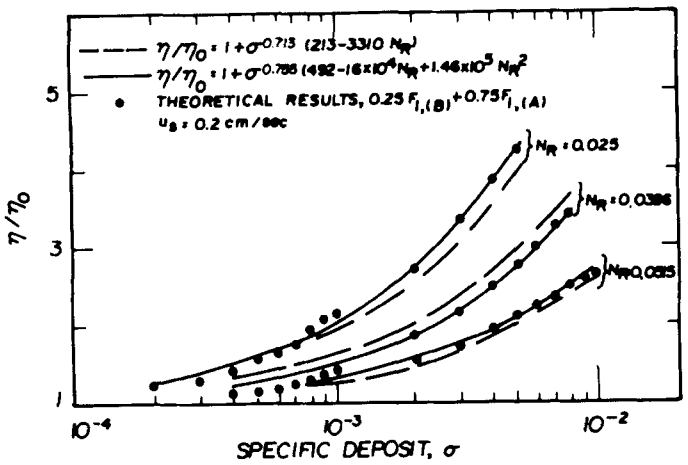

Figure 11. Correlation equation based on $(0.25F_{1,(B)} + 0.75F_{1(A)})$.

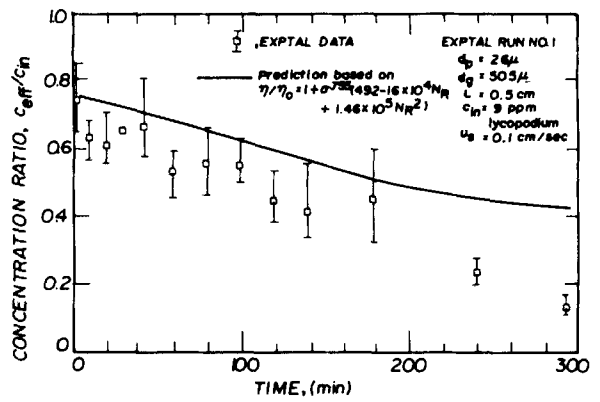

Figure 12a. Comparison of correlation equation with experimental data: Run No. 1.

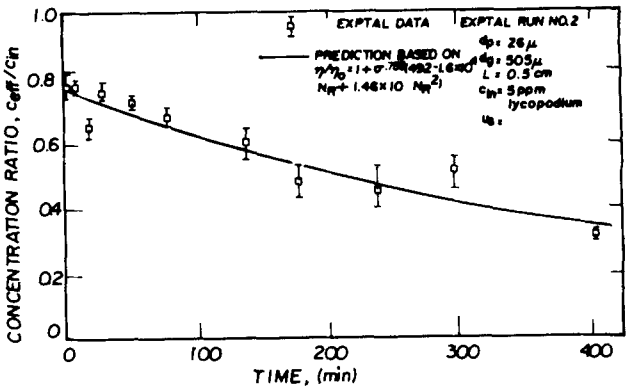

Figure 12b. Comparison of correlation equation with experimental data: Run No. 2.

were combined according to Eq. 19 to obtain F_1's as shown in Figure 11; as an approximation, these results can be represented by either of the following two expressions:

$$F_1 = \eta/\eta_o = 1 + \sigma^{0.713}(213 - 3{,}310N_R) \qquad (21a)$$

or

$$F_1 = \eta/\eta_o = 1 + \sigma^{0.755}(492 - 1.6 \times 10^4 N_R + 1.46 \times 10^5 N_R^2) \qquad (21b)$$

The agreement between either of these approximate expressions (i.e., Eqs. 21a and 21b) with the calculated results according to Eq. 19 can be seen in Figure 12. Generally speaking, both expressions give acceptable results. Equation 21b, however, gives better accuracy than Eq. 21a.

VALIDATION OF THE CORRELATION

The validity of the proposed correlation for the increase in filter coefficient resulting from particle deposition (F_1 vs. σ) is tested by comparing predicted histories of filtrate quality with experimental results obtained in the work as well as those reported earlier and listed in Table 4. The prediction was made by solving the phenomenological equations of filtration (namely, Eqs. 1 and 2 with boundary and initial conditions of Eq. 4 of Part I) using F_1 given by Eq. 21a or 21b. The results of these comparisons are summarized as follows.

1. Comparison with Experimental Data Obtained in This Work. Comparisons of predicted concentration ratio with experimental data obtained in this work are shown in Figure 12 for run Nos. 1 and 2. For run No. 1 predicted values of concentration ratio are higher than those of experimental data. As stated earlier, the empirical expression F_1 (Eq. 21a or 21b) was obtained using a combination factor, $f = 0.25$. The selection of $f = 0.25$ underestimates the increase in η for this run, as shown in Figure 10. The discrepancy in this case therefore can be expected. Agreement for experimental run No. 2, on the other hand, is very good. This good agreement is consistent with the fact that a combination factor of 0.25 fits the experimental data rather well, as Figure 10 shows.

2. Comparison with Tanaka's Data. Tanaka (1982) performed an extensive study of the effect of polyelectrolyte on filter performance. Among the results he obtained were several runs in each of which the time-dependent behavior of effluent quality at three depths of filter [i.e., 5, 12, and 20, in (127, 305, and 508 mm)] was presented. The major difference in experimental conditions among these four runs is the flocculent (polyelectrolyte) used. The effect of the polyelectrolyte can be seen from the zeta potential values shown in Table 4.

Comparisons of the effluent quality of two of the experimental runs with predictions are shown in Figure 13.

In making these comparisons it was necessary to assume an average particle size, which was taken to be the median diameter of 8.5 μm. The kaolin suspension used by Tanaka covered a wide size range, with 90% (by volume) of particles in the range of 4 to 19 μm. These two cases represent, respectively, the best and worst agreement observed. For the latter case, the correlation of Eq. 21b obviously underestimates the enhancement of λ resulting from particle deposition. Furthermore, this underestimate was more pronounced for large bed height and/or at times when the extent of deposition was significant.

3. Comparison with the Results of Vigneswaran, and Adin and Rebhun. Vigneswaran (1980) conducted filtration experiments using beds of greater height (30 cm) than were used in this study, and fairly large grains (up to 0.4 cm, nearly one order of magnitude greater than that used here). A systematic comparison was made between his experiments and prediction of the effluent concentration history based on Eq. 21b. Two cases of comparison, corresponding to the best and worst agreement observed, are shown in Figure 14. It should be noted that most of the other cases displayed agreement similar to that of Figure 14a rather than that of Figure 14b. The agreement, on the whole, can be viewed as satisfactory.

Another comparison between prediction of effluent quality

TABLE 4. EXPERIMENTAL CONDITIONS USED IN THIS WORK AND BY VIGNESWARAN, TANAKA, AND ADIN AND REBHUN

Experimenter and Run No.	Particles in suspension	d_p^* cm	d_g cm	u_s cm/s	Flocculant used	Zeta potential of particles mv
This work						
1	Lycopodium	0.0026	0.0505	0.1	None	−37
2	Lycopodium	0.0026	0.0505	0.2	None	−37
3	Lycopodium	0.0026	0.0505	0.27	None	−37
4	Lycopodium	0.0026	0.0505	0.4	None	−37
5	Ragweed	0.00195	0.0505	0.1	None	−17
Vigneswaran (1980)						
1	Broussonetia	0.0013	0.25	0.139	WAC-2	Not Avail.
2	Cuppressus Arizonica	0.0026	0.25	0.139	WAC-2	NA
3	Sorgho	0.0042	0.25	0.139	WAC-2	NA
4	Broussonetia	0.0013	0.4	0.139	WAC-2	NA
5	Cuppressus Arizonica	0.0026	0.4	0.139	WAC-2	NA
6	Sorgho	0.0042	0.4	0.139	WAC-2	NA
7	Broussonetia	0.0013	0.25	0.139	WAC-2	NA
8	Broussonetia	0.0013	0.25	0.278	WAC-2	NA
9	Broussonetia	0.0013	0.25	0.139	WAC-2	NA
Tanaka (1982)						
41	Kaolin	0.00085	0.17	0.3	5 mg/L of PDADMAC 587C	−9.4
19	Kaolin	0.00085	0.17	0.3	5 mg/L of PDADMAC 585C	−6
30	Kaolin	0.00085	0.17	0.3	1 mg/L of PEI P-600	−12.4
16	Kaolin	0.00085	0.17	0.3	3 mg/L of PEI P-150	−11
Adin and Rebhun (1974)	Kaolin	0.00085**	0.121	0.278	Cationic polymer	NA

* Size distributions of particles used in this work and by Vigneswaran are very narrow and can be considered as monodisperse. For kaolin particles used by Tanaka 90% (in volume) are in the size range of 4–19 μm; the median diameter is 8.5 μm.

** Size distribution of Kaolin particles used by Adin & Rebhun was not given; the value is assumed to be the same as that of Tanaka's.

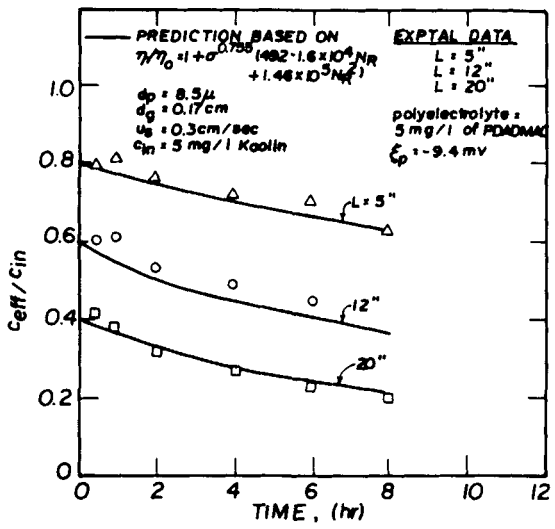

Figure 13a. Comparison of correlation equation with experimental data of Tanaka (1982): Run No. 41.

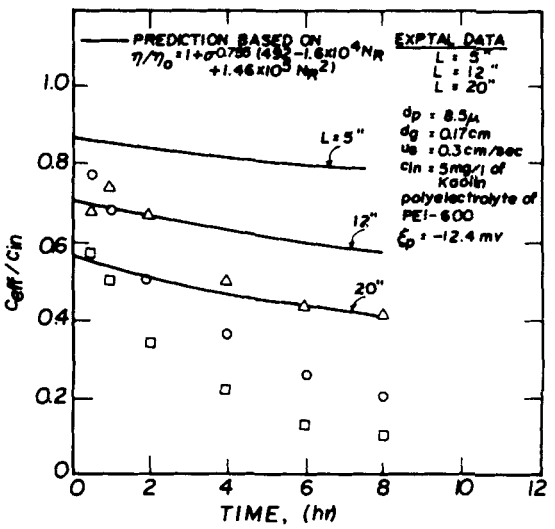

Figure 13b. Comparison of correlation equation with experimental data of Tanaka (1982): Run No. 30.

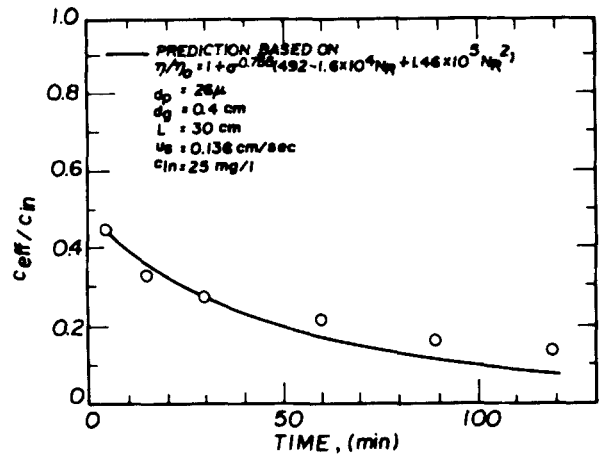

Figure 14a. Comparison of correlation equation with experimental data of Vigneswaran (1980): Run No. 5.

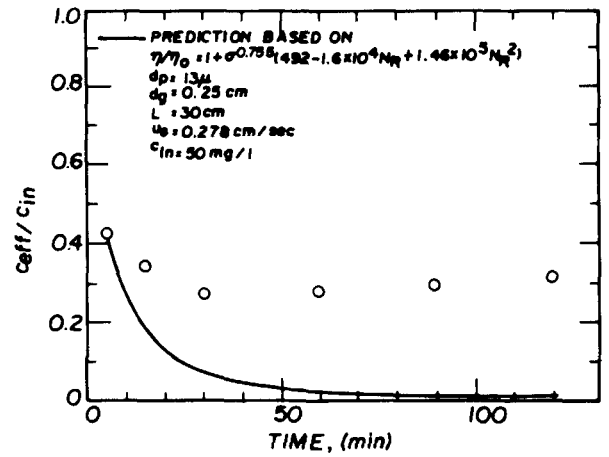

Figure 14b. Comparison of correlation equation with experimental data of Vigneswaran (1980): Run No. 8.

based on Eq. 21b and the results reported earlier by Adin and Rebhun (1974) is shown in Figure 15. Other than for the case of high bed height, the lack of agreement was obvious. The predictions were made on the assumption that the kaolin particle distribution was the same as that in Tanaka's work, an assumption unjustified but necessary because Adin and Rebhun did not provide any information on particle distribution.

In assessing the comparison results, two questions remain to be answered. First: How does one explain the disagreement observed? And second, and perhaps more important: What are the conditions under which Eq. 21b can be used for predicting the effluent concentration of deep bed filters? The greatest lack of agreement was found with the data of Adin and Rebhun. One was forced, in this case, to arbitrarily assume a size distribution for the suspension used for filtration, which undoubtedly introduced errors. In addition, the phenomenological equations (Eqs. 1 and 2 of Part I) used for predicting effluent concentration are for monodispersed suspension. Extension of these equations to polydispersed suspensions inevitably introduces inaccuracies the extent of which cannot be predicted with reasonable precision at present.

The correlation of Eq. 21b was based on experimental results obtained in this study. Its derivation, however, also incorporates the use of theoretical results. Thus, one may argue that its validity extends beyond the condition used in the experimental work. This

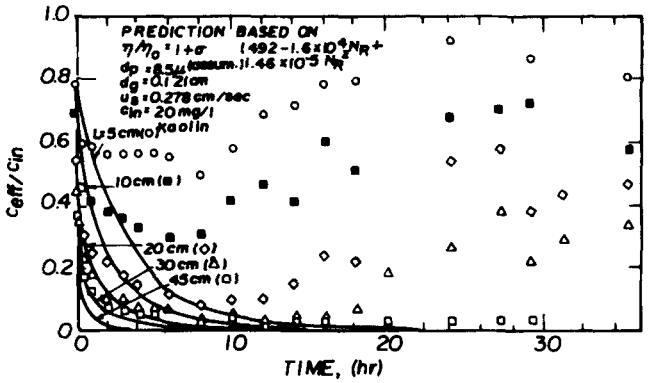

Figure 15. Comparison of correlation equation with experimental data of Adin and Rebhuhn (1974).

claim can be justified by the fact that, unlike earlier empirical correlations, Eq. 21b demonstrates the explicit effect of operating variables (through the dependence of F and N_R) as well as the substantial agreement between predictions and experiments reported from these independent sources. The present correlation, however, is not without deficiencies, principally:

(a) The omission of the effect caused by reentrainment of deposited particles, the importance of which can be seen, at least in certain cases, from the experimental results shown in Figure 15; and

(b) The effect of surface interaction, especially that resulting from the addition of polyelectrolyte between filter grains and suspended particles and between suspended particles themselves.

Concerning the latter deficiency, the nature of surface interaction is commonly characterized by the electrophoretic mobility measurement of the particle to be removed and the filter grains and is classified as favorable (i.e., attractive surface interaction) or adverse (i.e., repulsive surface interaction). In the context of the present study, the nature of the surface interaction may be considered as favorable (otherwise, the suspension becomes unfilterable, which should not occur in a well-designed system). Even though different types of surface interactions may all be favorable, they may however lead to the formation of particle deposits of different geometries. Consequently, one may argue that the combination factor, f of Eq. 18, should not be constant but is, instead, dependent upon the surface interaction between particles and filter grains and between particles themselves. The possibility of obtaining F_1 to incorporate the effect of surface interaction is currently being pursued.

ACKNOWLEDGMENT

This study was conducted under National Science Foundation Grant No. CPE-81-10760.

NOTATION

Only those terms not defined on Part I are given below.

A_s = Happel's model parameter
c_{eff} = effluent particle concentration
c_{in} = influent particle concentration
f = a combination factor defined by Eq. 18

$F_{1,(A)}$ = theoretical value of F_1 based on limiting case (A)
$F_{1,(B)}$ = theoretical value of F_1 based on limiting case (B)
$F_{1,expt}$ = experimentally determined value of F_1
Ha = Hamaker constant
N = (L/ℓ)
N_G = $2(\rho_p - \rho)a_p^2 g/(9\mu u_s)$, dimensionless gravitational group
N_{Lo} = $Ha/(9\pi\mu a_p^2 u_s)$, London parameter
N_{Pe} = $u_s d_g/D$, Peclet number
w_m = weighting factor

Greek Letters

η_i = collection efficiency of the ith collector
η_{i_o} = initial collection efficiency of the ith collector
ϕ_n = specific deposit in the nth unit collector
ϕ_c = objective function, see Eq. 11
ϕ_p = objective function, see Eq. 15

LITERATURE CITED

Only those sources not listed in Part I are given below.

Adin, A., and M. Rebhun, "High Rate Contact Flocculation-Filtration with Cationic Polyelectrolytes," *J. Amer. Water Works Assoc.*, **66**, 109 (1974).

Rajagopalan, R., and C. Tien, "The Theory of Deep-Bed Filtration," *Progress in Filtration and Separation*, R. J. Wakeman, Ed., Elsevier, Amsterdam, **I**, (1979).

Tanaka, T. S., "Critical Parameters Influencing the Filtration Kinetics of a Low Turbidity Water Supply," Ph.D. Dissertation, Univ. of Southern California, Los Angeles, CA (1982).

Vigneswaran, S., "Contribution a la Modelisation dans la Masse," D. Eng. Thesis, Fac. Sci., Montpellier, France (1980).

Manuscript received Feb. 16, 1984; and accepted Nov. 24, 1984.